Asian Journal of Green Chemistry 8 (2024) 25-38

Asian Journal of Green Chemistry

Original Research Article

View Article Online | View Journal

Silver Nanoparticles Synthesized Using *Ageratum conyzoides* Leaf Extract Exhibit Antioxidant, Anti-inflammatory and α-Glucosidase Inhibitory Properties

Jimoh Olamilekan Igbalaye[a,*], Adesegun Gideon Adeyemo[a], Adetola Olajumoke Adenubi[a], Oladejo Ahmodu[a], Basit Opeyemi Shodimu[a], Faizat Olasumbo Hazeez[a], Suliat Adenike Hassan[b]

[a]*Biochemistry Department, Faculty of Science, Lagos State University, Ojo, PMB 0001, Lagos, Nigeria*

[b]*Physiology Department, Faculty of Basic Medical Sciences, Ladoke Akintola University of Technology, Ogbomosho, Nigeria*

ARTICLE INFORMATION

Submitted: 31 May 2023
Revised: 12 August 2023
Accepted: 16 August 2023
Available online: 26 August 2023

Manuscript ID: AJGC-2305-1396
Checked for Plagiarism: Yes
Language Editor:
Dr. Fatimah Ramezani
Editor who approved publication:
Dr. James Bashkin

DOI: 10.48309/ajgc.2024.399046.1396

KEYWORDS

Silver nanoparticles
Ageratum
Antioxidant
Anti-inflammatory agent
α-Glucosidase

ABSTRACT

Silver nanoparticles (AgNPs) synthesis has attracted a growing attention with an increasing focus on the production of nanoparticles of biomedical importance through ecofriendly means. This study assessed the antioxidant, anti-inflammatory, and α-glucosidase inhibitory potentials of AgNPs synthesized using *Ageratum conyzoides* aqueous leaf extract *in vitro*. The extract's phytoconstituents were determined by GC-MS analysis. AgNPs was synthesized by mixing $AgNO_3$ solution with the aqueous leaf extract of *A. conyzoides*. AgNPs formation was monitored by UV-Visible spectrophotometry. The obtained AgNPs was further characterized using SEM and FT-IR analysis. Antioxidant potential was evaluated via ferric reducing power, hydrogen peroxide, and ABTS scavenging assays. Anti-inflammatory capacity of the synthesized AgNPs was assessed through inhibition of trypsin activity and albumin denaturation. Furthermore, anti-diabetic potential was evaluated by α-glucosidase inhibitory activity of the AgNPs, all in comparison with controls and standards. GC-MS analysis reveals Oleic acid (25.90%), Oxalic acid, allyl hexadecyl ester (25.49%) and Dodecanoic acid (13.36%) as the main phytoconstituents in *A. conyzoides* extract. The UV-Visible analysis detected the absorption peak of AgNPs at 420 nm. SEM reveals various morphological forms of the AgNPs i.e. spherical and triangular. The average particle size is 27.85 nm. FTIR analysis showed that the plant phytoconstituents capped and stabilized the synthesized AgNPs. The AgNPs showed substantial ferric reducing power in addition to hydrogen peroxide, DPPH, and ABTS radicals scavenging activities while also inhibiting albumin denaturation, trypsin, and α-glucosidase activities. These findings revealed the suitability of *Ageratum conyzoides* for AgNPs synthesis and also demonstrated the potentials of the synthesized AgNPs as an antioxidant, anti-inflammatory, and anti-diabetic agent.

Corresponding authors, email: jimoh.igbalaye@lasu.edu.ng (J.O. Igbalaye).
Tel.: 2348062479139.

Graphical Abstract

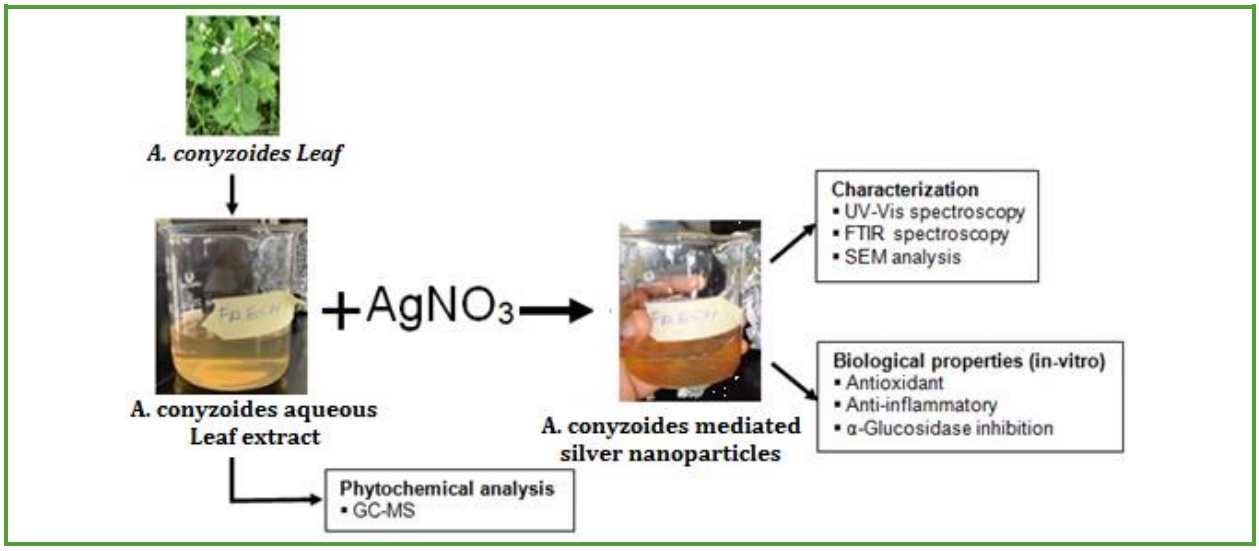

Introduction

Nanomaterials synthesis is gaining increased attention due to their unique properties, which are absent in bulk materials. The form and size of nanoparticles influence the behavior of nanomaterials, which is a crucial factor in nanoparticles application [1]. Several metallic salts, including silver (Ag), are utilized to produce metal nanoparticles. Silver nanoparticles (AgNPs) have numerous advantages over other various metallic nanoparticles. Owing to their high chemical stability, silver nanoparticles are reported to possess excellent capacitance properties, electron transfer capabilities, and electro catalysis [2]. Some include a significant quantity of Ag_2O despite the fact that many are classified as AgNPs due to their high surface to bulk Ag atom ratio. AgNPs have been applied in a variety of electronic and medical devices, surgical tools, bone cements, and antimicrobial agents, amongst other applications [3-5]. In addition, AgNPs have been deployed as wound and burn treatment agents [6-8]. AgNPs have also been employed as molecular labelling tools due to their large scattering cross-sections and surface plasmon resonance [9]. Different AgNPs variants are now being identified for their diverse potential applications [10, 11]. The biological process of nanoparticle production is favored over physical and chemical methods because it avoids the use of potentially dangerous chemicals and irradiations [12]. Meanwhile, plant-mediated green synthesis of nanoparticles has recently emerged as the preferred biological synthetic route due to the tedious processes of procurement, isolation, purification, and maintenance of microbial cultures, in addition to the high cost of nutrient media [13]. Other problems that make microbes and algae less desirable than plants include culture contamination and less well-known bio-capping chemicals. As a result, bio-nanotechnologists prefer the production of silver and other metallic nanoparticles using plants and their byproducts since it is rapid, inexpensive, environmentally benign, and non-pathogenic. Moreover, green methods give a great yield of nanoparticles production with high reproducibility [14]. The various

phytochemicals present in plants play significant roles as reducing and stabilizing agents in the phytosynthesis of nanoparticles [15-17].

Ageratum conyzoides L. is a common invasive weed in and around Indian agro-ecosystems, particularly in the Indo-Gangetic plains and Narmada basin and belongs to the Asteraceae family. The plant is very adaptable to many ecological situations and exhibits morphological variants. Alkaloids, flavonoids, chromenes, benzofurans, and terpenoids are just a few of the chemical substances that have been identified in this species [18]. There have been reports that the extracts and metabolites of this plant possess hypoglycemic, anti-inflammatory, antimalarial, anti-protozoal, fungicidal, and insecticidal activities [19]. We hypothesized that the medicinal properties of this plant can be enhanced when coupled to a particle of larger surface area. Therefore, this study aimed to synthesize AgNPs from the aqueous leaf extract of *Ageratum conyzoides*, and assess its *in vitro* antioxidant, anti-inflammatory, and anti-diabetic properties.

Experimental

Preparation of Ageratum conyzoides extract

Ageratum conyzoides leaves were gotten from a field in Ojo, Lagos, Nigeria. The leaves were blended using a grinder. 8% (w/v) of the aqueous extract of *Ageratum conyzoides* was prepared in a 500 ml conical flask holding 8 g of the powdered leaf and 100 mL of deionized water and heated at 70 ^{o}C for 2 h. Following a 5-minute centrifugation at 3000 rpm, the mixture was then filtered using Whatman No. 1 filter paper. The filtrates were further centrifuged at 3000 rpm for 5mins to get a clear solution, which was then stored in the refrigerator for further usage.

Determination of phytochemical constituents

GC-MS analysis of the filtrate obtained from the aqueous leaf extract of *Ageratum conyzoides* was conducted using an Agilent 5977B GC/MSD system (Agilent Co., United States) coupled with Agilent 8860 auto-sampler, equipped with an HP-5MS Ultra Inert (5% diphenyl / 95% dimethylpolysiloxan) fused to a capillary column (30 m × 250 µm ID × 0.25 µm df). For detection, an electron ionization system was run in electron impact mode with an ionization energy of 70 eV Helium (99.999%) was used as the carrier gas at a constant flow rate of 1 mL/min. The GC-MS was programmed as thus: injector port temperature was set to 325 ^{o}C, interface temperature set as 250 ^{o}C and the ion-source maintained at 250 ^{o}C. The oven temperature was set as a variable (50 ^{o}C for 2 min, 180 ^{o}C at 5 ^{o}C/min, up to 270 ^{o}C at 20 ^{o}C/min), split ratio was set as 1:50, and the splitless mode injector was used. Mass spectra were taken at 70 eV, the MS was set to scan from 40 to 500 Da. The GC-MS mass spectrum was interpreted employing the National Institute Standard and Technology (NIST) and the National Centre for Biotechnology Information databases. Comparison was made between the spectra of the unknown components and the spectrum of known components stored in the NIST collection. Structures of the predominant phytoconstituents were drawn using ChemDraw (version 12.0.2).

Synthesis and characterization of silver nanoparticles

10 mL solution was prepared using 1 mL extract and 9 mL of 0.001M silver nitrate. The mixture was kept in a dark room. Synthesis was monitored by checking the absorbance at one-hour interval for 5 hours, using UV-Visible spectrophotometer (Uniscope, SM-7504,

Surgifriend Medicals, England) at 200-700 nm wavelength. At the end of the reaction, the solution (extract + reduced silver nitrate, AgNPs) was centrifuged at 5000 rpm for 15 mins, and the pellet was gathered and dried in the oven at 80 °C for 1 h [20]. Scanning electron microscopy (SEM) (JEOL, JSM-7600F, Tokyo, Japan) was used in determining the morphological features of the synthesized AgNPs. Fourier Transform Infrared (FT-IR) analysis (Cary 630, Agilent, USA) was utilized to identify the functional groups coating the surface of the formed AgNPs.

Antioxidants activity determination

ABTS assay

Concisely, 2.45 mM potassium persulphate in deionized water was mixed with 7 mM ABTS solution and allowed to incubate for 16 h. The solution was diluted after incubation till the absorbance read 0.7 at 743 nm. 200 µl of the resulting ABTS working solution was added to 5 µL of test sample, allowed to stand at room temperature for 6 minutes and then absorbance was taken at 734 nm [21] against an ethanol blank, using ascorbic acid as standard. The scavenging activity, expressed as percentage, was computed using the following equation:

$$\%Activity = \frac{A_C - A_s}{A_{C\times 100}} \qquad (1)$$

Where, A_c is the control absorbance (all the reagent except the test sample) and A_s is absorbance of sample/Ascorbic acid.

Hydrogen peroxide scavenging activity

This was performed according to Keshari [22]. 0.1 mL of test sample in phosphate buffer (50mM, pH = 7.4) was added to 0.3 mL phosphate buffer (50 mM, pH 7.4) and 0.6 mL hydrogen peroxide solution (2 mM H_2O_2 in phosphate buffer, 50 mM, pH 7.4). The resulting solution was vigorously mixed, and the absorbance was recorded after 10 min at 230 nm. Ascorbic acid was utilized as standard and phosphate buffer (50 mM, pH 7.4) as blank. The percentage of hydrogen peroxide scavenging activity was calculated using Equation (1).

Reducing power activity

In brief, 2.5 mL test samples were added to 2.5 mL of phosphate buffer (200 mM, pH 6.6) and 2.5 mL of 1% potassium ferricyanide. The resulting mixture was incubated at 50 °C for 20 min and allowed to cool. Afterwards, the mixture was centrifuged at 3000 rpm for 8mins following the addition of 2.5 mL 10% trichloroacetic acid. The obtained supernatant was then mixed with equal quantity of deionized water. Lastly, 1 mL of 0.1% ferric chloride was then added to the upper layer and the absorbance was read spectrophotometrically at 700 nm [23]. BHT was employed as standard. The reducing power percentage was calculated using Equation (1).

DPPH radical scavenging assay

DPPH radical scavenging activity of the synthesized AgNPs was evaluated following a previously reported method [22] with slight adjustments. 2.4 mg of DPPH is dissolved in 100 mL of methanol to create a DPPH radical solution. 5 µl of test sample was mixed with 3.995 ml of methanolic DPPH. The assay mixture was vortexed and incubated at room temperature in the dark for 30 min. Absorbance was taken spectrophotometrically at 515 nm. The DPPH radical solution was used as blank. The DPPH radical activity was estimated using Equation (2):

$$DPPH\ scavenging\ activity\ (\%) = \frac{A_b - A_a\ /A_b}{100} \qquad (2)$$

Where, A_b is absorbance of blank at t = 0 min, A_a is absorbance of sample at t = 30 mins. A standard curve was plotted with scavenged DPPH (%) against vitamin C concentration.

In vitro anti-inflammatory assay

Trypsin inhibitory activity of AgNPs

The assay was conducted following the methods of Oyedepo [24] and Sakat [25] with modifications. 0.06 mg of trypsin was added to 1 mL of 20 mM Tris HCl buffer (pH 7.4) and 1 ml of test samples to make a total reaction mixture of 2 mL. The resulting mixture was incubated at 37 °C for 5 min after which 1 mL 0.8% (w/v) casein was added. To halt the rection, 2 mL of 70% perchloric acid was introduced to the mixture after an additional 20 min of incubation. The resulting cloudy suspension was centrifuged, and the supernatant absorbance was measured at 210 nm versus a buffer blank. The percentage inhibition of trypsin activity was determined using Equation (1).

Inhibition of protein denaturation

The test was conducted following the protocol of Varghese and Mathew [26]. Briefly, 1% bovine serum albumin (BSA) stock was prepared using deionized water. The assay mixture contained 0.5 mL of BSA and test samples and was incubated for 15minutes at room temperature. Denaturation was caused by heating the reaction mixture at 60 ^{o}C for 10 min, after which absorbance was taken at 660 nm. Aspirin was used as standard and BSA only containing solution as the control. The percentage inhibition of denaturation was calculated using Equation (1).

α–Glucosidase inhibitory activity

Inhibition of ∝- glucosidase was assayed following the modified method of Kim *et al.* [27]. The reaction mixture, containing 150 µl of 0.1 M sodium phosphate buffer (containing 6 mM NaCl, pH 6.9), 0.1 units of ∝-glucosidase, and 50 µl of test samples, which was pre-incubated at 37 °C for 10 minutes, and then 25 µl of 2 mM para-nitrophenyl-∝-D-glucopyranoside in 25 µl 0.1 M sodium phosphate buffer was added to the mixture and incubated for additional 20 minutes at 37 °C. 50 µl of 0.1 M sodium carbonate (Na_2CO_3) was then added to terminate the reaction and absorbance was read at 405 nm. Acarbose was used as standard, and the ∝-glucosidase solution lacking the test sample served as the control. Percentage ∝-glucosidase inhibition was calculated using Equation (1).

Statistical analysis

Data obtained were subjected to statistical analysis. Spectra data were plotted using MS Excel. Using SPSS version 20, One-way ANOVA and the Tukey multiple comparison test were employed in making group comparisons. Values are presented in bar charts as mean±SEM with statistical significance obtained at $p < 0.05$.

Results and Discussion

Phytochemical composition

The phytochemical constituents of the aqueous leaf extract of *Ageratum conyzoides* as revealed by GC-MS analysis is presented in Table 1. Of the twenty-five different phytochemicals identified in *Ageratum conyzoides* aqueous leaf extract, the three

predominant components are Oleic acid (25.90%), Oxalic acid, allyl hexadecyl ester (25.49%), and Dodecanoic acid (13.36%), which are the likely main contributor to the plant's biological activities. Moreover, oleic acid, a monounsaturated fatty acid, has been demonstrated to possess antioxidant, anti-inflammatory and antitumor effects [28, 29]. The chemical structure of the three major phytoconstituents identified in the aqueous leaf extract of *Ageratum conyzoides* are displayed in Figure 1.

Synthesis and characterization of silver nanoparticles

The aqueous leaf extract of *Ageratum conyzoides* changed from yellowish-brown to dark brown on mixing with $AgNO_3$ solution within 5 hours (Figure 2a and 2b). This is as a result of the phytoactive chemicals present in the aqueous extract of *Ageratum conyzoides*, which caused the reduction of Ag^+ to Ag^0 [23]. There was no further color change after 24 hours. Previous studies have demonstrated that phenolic compounds are highly potent as reducing agent for nanoparticles formation [30]. As seen in Figure 2c, the UV-Visible spectra substantiate the AgNPs formation.

Table 1. Phytochemicals identified in the aqueous leaf extract of *Ageratum conyzoides*

No.	RT (min)	Name of compound	Peak Area %	Molecular formula	MW g/mol
1	5.51	Oxalic acid, allyl hexadecyl ester	25.49	$C_{21}H_{30}O_4$	354.50
2	6.13	8-Oxabicyclo[5.1.0]octane	1.62	$C_7H_{12}O$	112.17
3	6.44	Cyclohexane, 1,2-dimethyl-, cis-	6.84	C_8H_{16}	112.21
4	9.77	Decane, 2,9-dimethyl-	0.15	$C_{12}H_{26}$	170.33
5	14.90	2-Heptafluorobutyroxydodecane	0.24	$C_{16}H_{25}F_7O_2$	382.36
6	15.16	Decane	0.39	$C_{10}H_{22}$	142.28
7	17.70	Heptane, 2,6-dimethyl-	0.34	C_9H_{20}	128.25
8	18.09	2,4-Di-tert-butylphenol	1.24	$C_{14}H_{22}O$	206.32
9	19.00	N-(3-Methylbutyl)acetamide	0.91	$C_7H_{15}NO$	129.20
10	19.40	4,4,5,5,5-Pentafluoropentan-2-one	1.33	$C_5H_5F_5O$	176.08
11	20.09	Hexadecane	5.43	$C_{16}H_{34}$	226.44
12	20.90	Dodecanoic acid	13.36	$C_{12}H_{22}O_2$	200.32
13	22.36	Oxalic acid, allyl decyl ester	0.62	$C_{15}H_{26}O_4$	270.36
14	24.34	3,5-Di-tert-butylbenzoic acid	0.21	$C_{15}H_{22}O_2$	234.33
15	24.53	Oxalic acid, allyl decyl ester	0.23	$C_{15}H_{26}O_4$	270.36
16	28.38	3-Eicosene, (E)-	0.20	$C_{20}H_{40}$	280.50
17	28.50	Oxalic acid, allyl undecyl ester	0.15	$C_{16}H_{28}O_4$	284.39
18	29.52	Oleic Acid	0.25	$C_{18}H_{34}O_2$	282.50
19	29.83	Cycloeicosane	0.24	$C_{20}H_{40}$	280.50
20	30.43	Cyclohexadecane, 1,2-diethyl-	1.57	$C_{20}H_{40}$	280.50
21	31.64	1-Docosene	4.41	$C_{22}H_{44}$	308.60
22	31.78	1-Hexacosanol	0.66	$C_{26}H_{54}O$	382.70
23	32.25	Cycloeicosane	4.34	$C_{20}H_{40}$	280.50
24	32.60	3-Eicosene, (E)-	3.88	$C_{20}H_{40}$	280.50
25	33.19	Oleic Acid	25.90	$C_{18}H_{34}O_2$	282.50

RT: Retention time and MW: Molecular weight

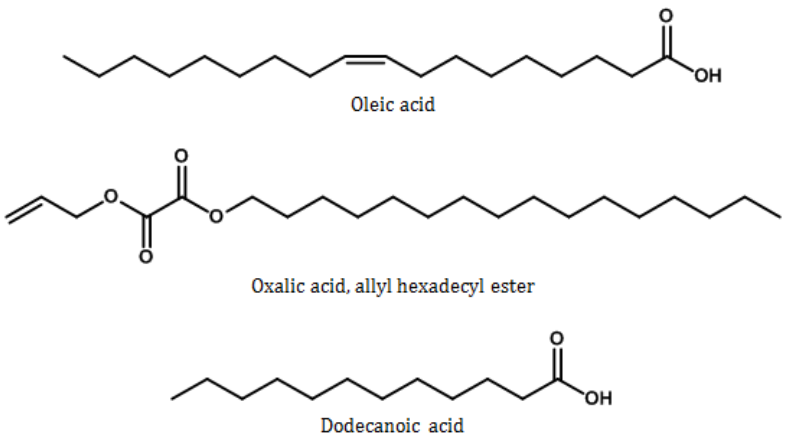

Figure 1. The chemical structure of the main phytoconstituents in *A. conyzoides* aqueous leaf extract

The UV-Visible absorbance spectra were recorded at the wavelength between 200-600 nm every 1hr interval for the next 5 hours (where there was no visible colour change). The maximum wavelength (λ_{max}) was around 400 nm. Likewise, several earlier researches have reported that the absorption spectrum between 410 and 450 nm observed in AgNPs is due to surface plasmon resonance [31].

Figure 3a and 3b show the morphological characteristics of the synthesized AgNPs by *Ageratum conyzoides* leaf extract which was shown to be relatively spherical. The SEM image of AgNPs resulted from the hydrogen bond and electrostatic interactions between the phytoactive capping and stabilizing molecules coating the AgNPs surface. The larger AgNPs may have resulted from the assembly of the smaller ones [32]. Figure 3c shows the size distribution pattern of the formed AgNPs. The SEM analysis confirmed that the formed AgNPs were of varied shapes (i.e. spherical, and triangular), and the size ranged from 10-50 nm.

Figure 4 shows the FT-IR spectrum of the formed AgNPs from the aqueous leaf extract of *Ageratum conyzoides*. FT-IR analysis is crucial for the detection of functional groups coating the surface of nanoparticles. The strong broad absorption peak at 3265.1 cm^{-1} could be ascribed to the O—H stretch of alcohol, the absorption peak at 2109.7 cm^{-1} resulted from the C≡C stretch vibrations of alkynes while the medium peak at 1636.3 cm^{-1} is assigned to N—C=O amide I bond of proteins [33]. The FT-IR results indicate that various functional groups of the phytochemicals in *Ageratum conyzoides* aqueous leaf extract are responsible for the capping and stabilization of the synthesized AgNPs.

Antioxidant activity

The antioxidant potential of the AgNPs synthesized from *Ageratum conyzoides* was evaluated using ferric reducing power, and their ability to scavenge hydrogen peroxide, ABTS, and DPPH radicals. As demonstrated in Figure 5a, the synthesized AgNPs had a greater ferric reducing power in comparison with the extract but not as compared to the standard Vitamin C. In a similar study, AgNPs synthesized from *Aesculus hippocastanum* possess more ferric ion reducing activity than the plant extract [33]. Figure 5b showed that synthesized AgNPs hydrogen peroxide scavenging activity was higher compared to the extract, with vitamin C showing the greatest activity.

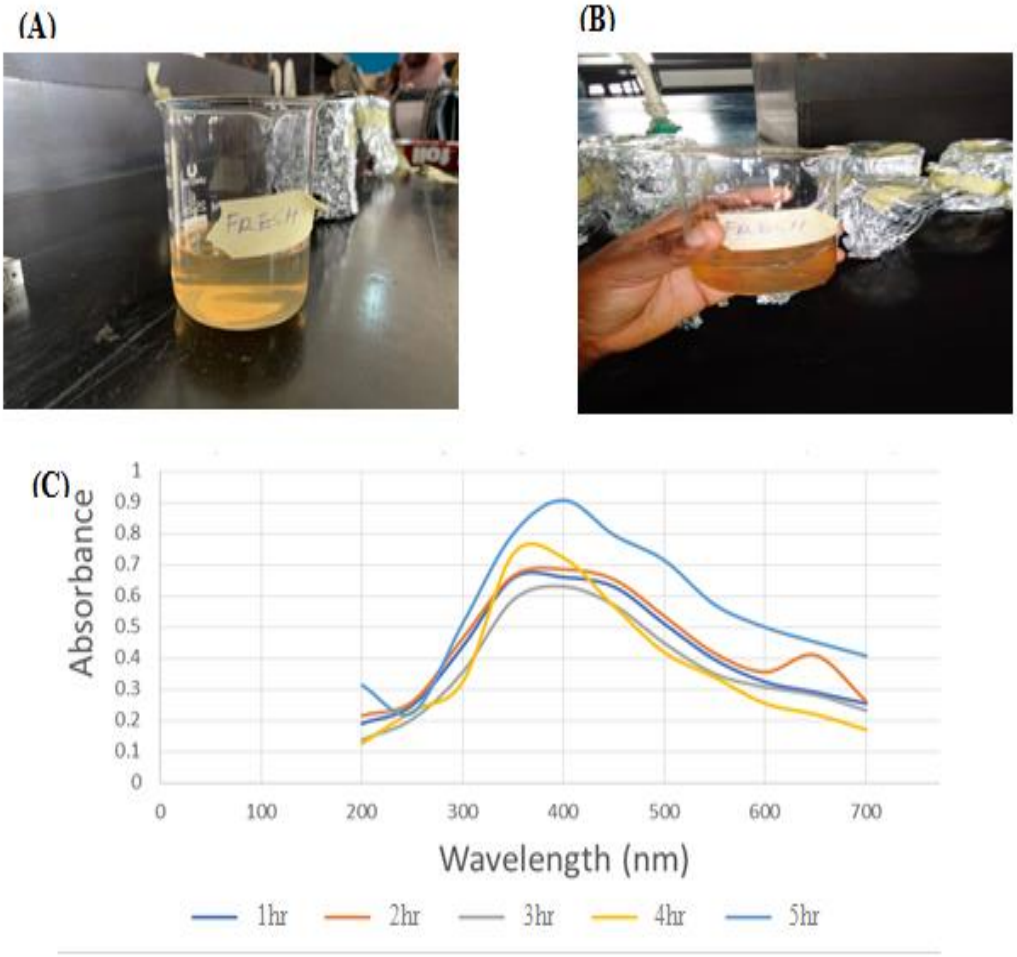

Figure 2. a,b) Visual observation of colour change in the extract and c) UV-Visible absorption spectra of the synthesized AgNPs obtained at various time gaps

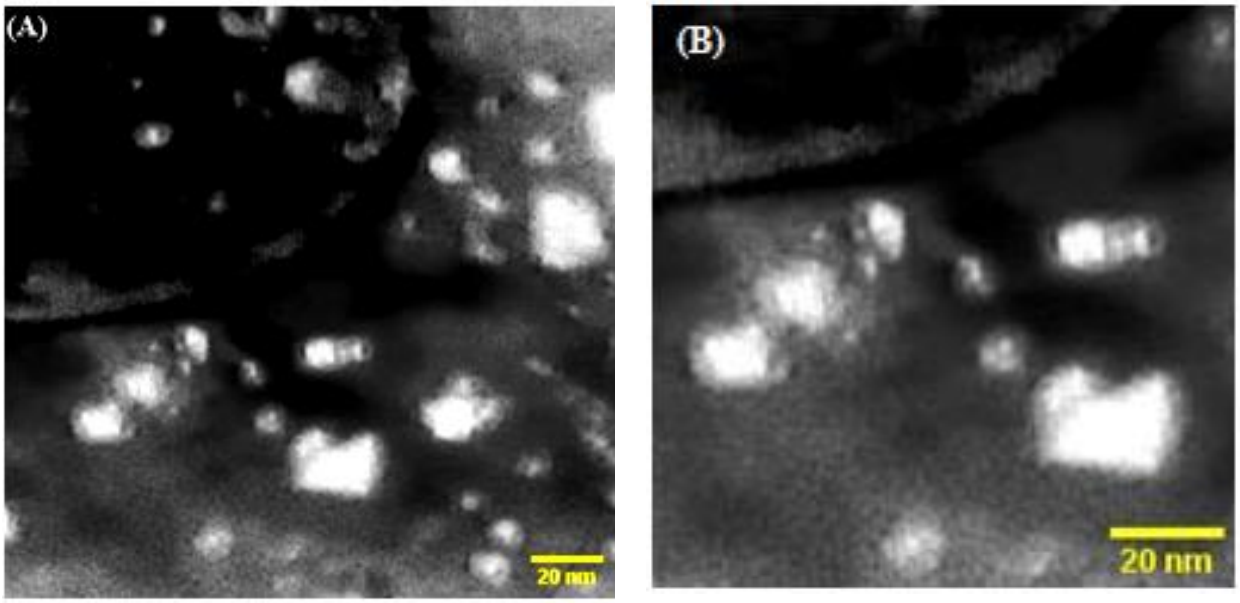

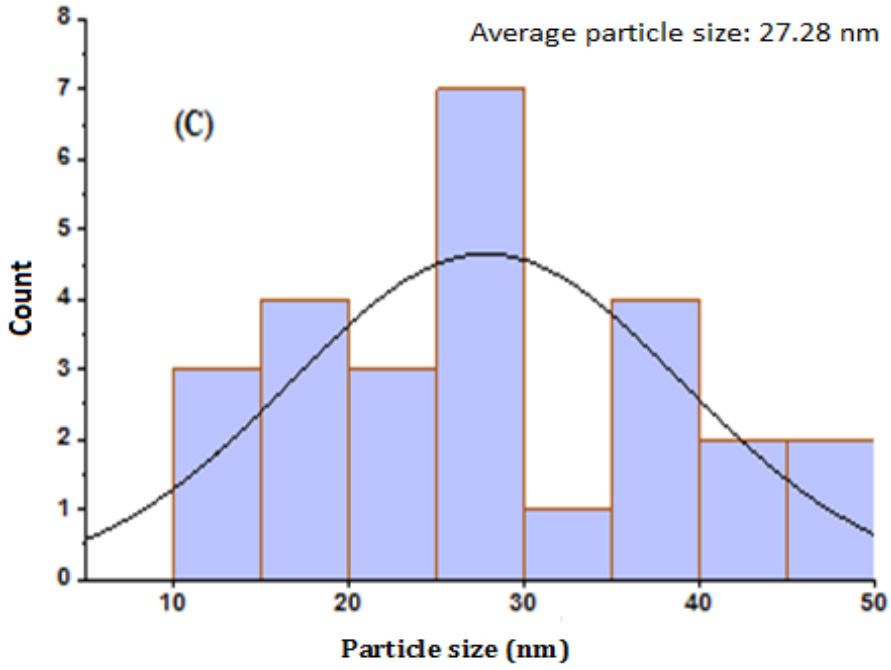

Figure 3. a,b) SEM images present the morphological features of the synthesized AgNPs at different magnifications and c) histogram show the size distribution pattern of the synthesized AgNPs

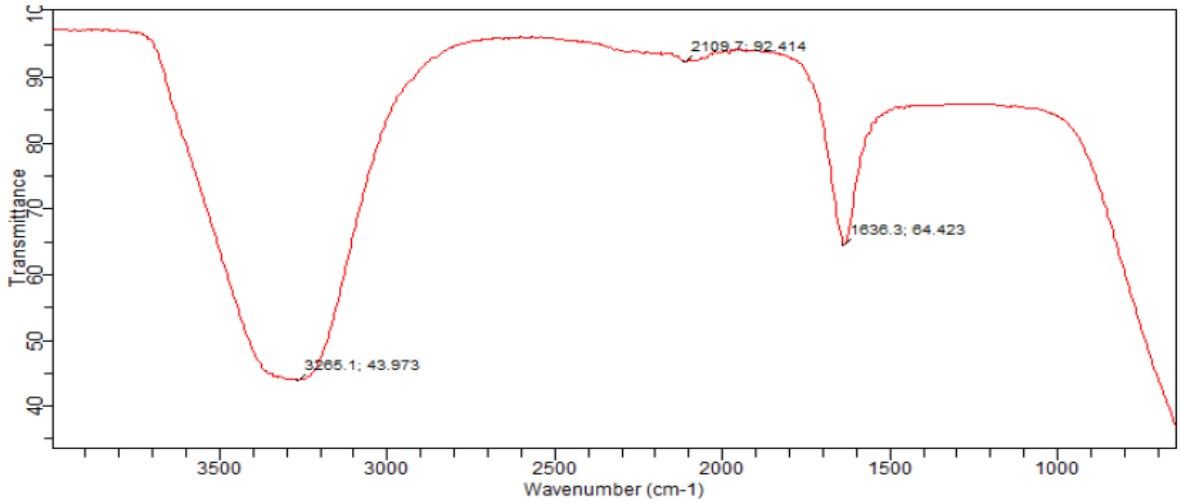

Figure 4. FT-IR spectrum of the synthesized silver nanoparticles (AgNPs)

These properties of silver nanoparticles arise due to the presence of the phytoconstituents-derived functional groups on their surface [33]. Similar results were published by Keshari [34] and Chick [35], where the antioxidant properties of *Cestrum nocturnum* and *Microsorum pteropus* derived silver nanoparticles were investigated respectively. Furthermore, the synthesized AgNPs exhibited the highest DPPH radical scavenging activity of about 80% when compared with the control and standard as seen in Figure 5c. Bharathi [36] reported similar activity for AgNPs synthesized from *Cassia angustifolia* flowers. The synthesized AgNPs in this study also showed high ABTS

radical scavenging activity, which was significantly higher than that of $AgNO_3$, extract, and vitamin C (Figure 5d). This result agrees with the findings of Moldovan [37] and Rajkumar [38], where the authors reported that biosynthesized silver nanoparticle exhibited significant ABTS scavenging activity. Oxidative stress, defined as an upsurge in the steady state level of reactive oxygen and nitrogen species, is thought to be caused by iron overload [39]. Hence, agents that are able to reduce iron overload could be mentioned to possess antioxidant properties. Furthermore, it is common practice to subject biological models to hydrogen peroxide (H_2O_2) exposure to induce oxidative stress/damage. The Fenton's reaction between H_2O_2 and Fe^{2+} ions generate the highly reactive OH^- radical, which is considered as the main mechanism for oxidative damage [40]. Therefore, the ability to eliminate hydrogen peroxide is an indication of antioxidant potential. Excessive free radicals are also known to be responsible for oxidative stress conditions. As such, a molecule is mentioned to exhibit antioxidant properties if it can eliminate or inactivating free radicals [41]. The observed ferric reducing power, hydrogen peroxide, ABTS, and DPPH radical scavenging activities of the AgNPs suggests its potential as an active antioxidant agent.

Anti-inflammatory activities

Inhibition of thermally induced denaturation of albumin and inhibition of trypsin activity assays were employed for the assessment of anti-inflammatory activity of the AgNPs synthesized from *Ageratum conyzoides* as earlier described. Figure 6a indicates that AgNPs has significantly higher albumin denaturation inhibitory activity when compared to the control and standard. Our findings are similar to that of Kedi [42] and Prabakaran [43], who reported that AgNPs synthesized from the extract of *Selaginella myosurus* and *Eichhornia crassipes* inhibited the denaturation of egg albumin. The AgNPs synthesized in this study was further observed to inhibit the activities of trypsin, which was significantly higher than that of the control (Figure 6b). The inhibitory activity could be due to the interference of AgNPs with the three-dimensional structure of trypsin or the blockage of its active site [44]. Inflammatory response usually involves the denaturation and degradation of proteins [45]. The observed inhibition of albumin denaturation and trypsin activity suggests the anti-inflammatory potential of the synthesized AgNPs.

α–Glucosidase inhibitory activity

The anti-diabetic potential of AgNPs synthesized from *Ageratum conyzoides* extract was assessed with alpha glucosidase inhibitory assay. Figure 7 illustrates that the synthesized AgNPs has inhibitory activity of above 80%, which is significantly higher than that of $AgNO_3$, *Ageratum conyzoides* extract and the standard (acarbose).

The inhibition observed in this study could be due to the disruption of the enzyme's three-dimensional structure or the blockage of the active site [46].

Silver nanoparticle synthesized from *Enhalusa coroides* and *Allium sepa* showed similar alpha glucosidase inhibitory activity [47, 48]. Diabetes is characterized by prolonged hyperglycaemia [49]. The reduction or inhibition of activities of enzymes involved in carbohydrates catabolism such as alpha glucosidase could help manage diabetic condition [50, 51]. This inhibition of alpha glucosidase observed in this study suggests that the synthesized AgNPs is a potential antidiabetic agent.

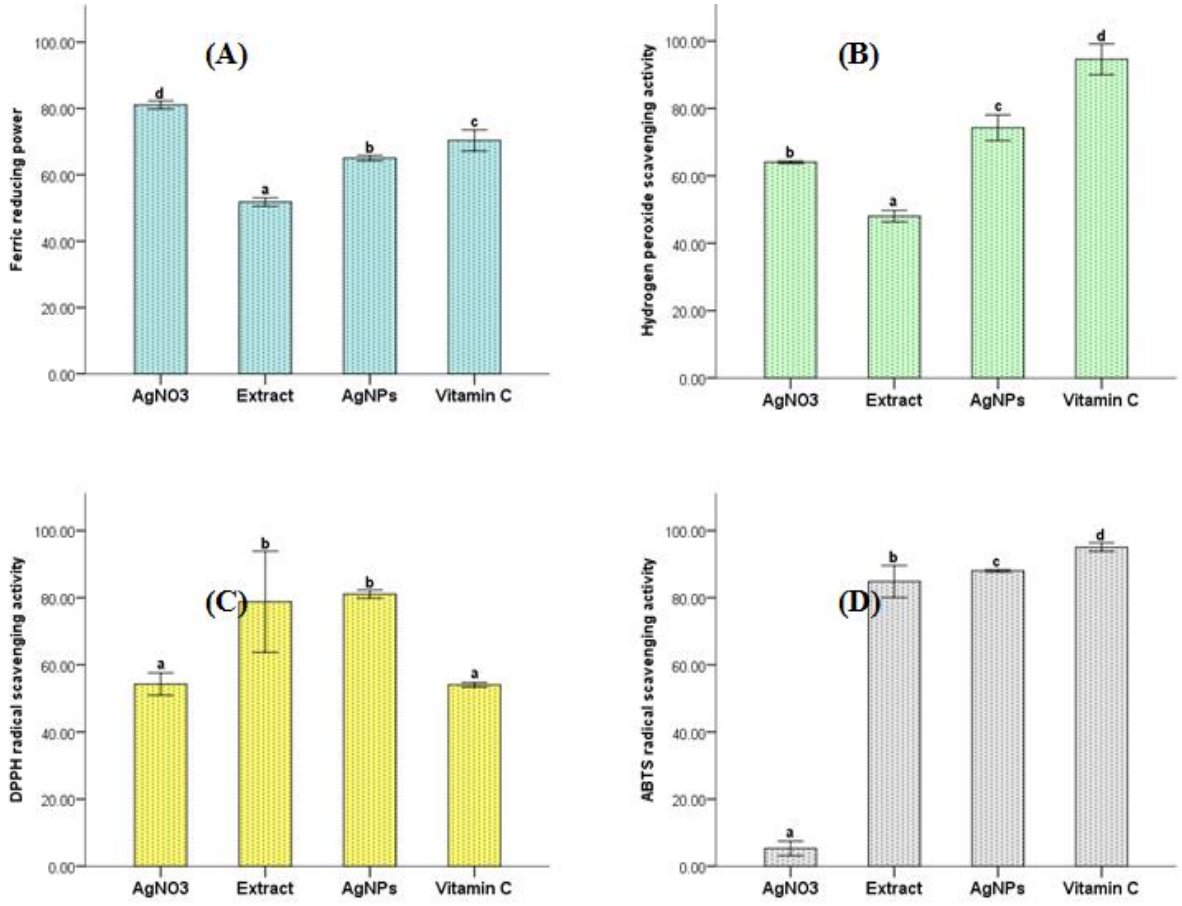

Figure 5. a) The ferric reducing power, b) hydrogen peroxide, c) DPPH, and d) ABTS radical scavenging activities of silver nitrate, *A. conyzoides* extract, and the synthesized AgNPs in comparison with vitamin C

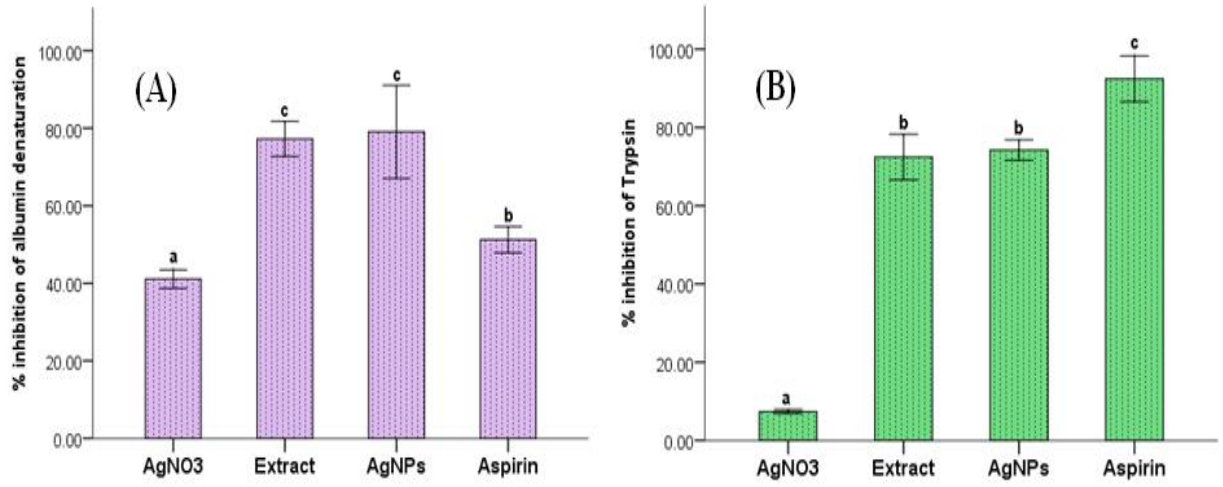

Figure 6. a) Inhibition of albumin denaturation and b) trypsin activity by silver nitrate, A. conyzoides extract and the synthesized AgNPs in comparison with a standard (aspirin)

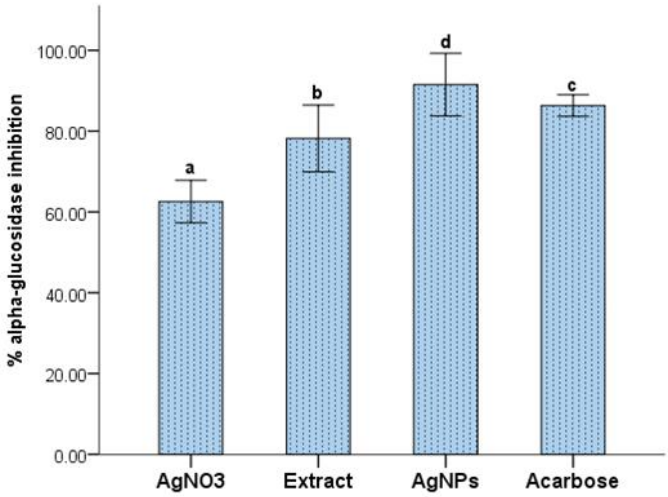

Figure 7. Inhibition of α-glucosidase by silver nitrate, *A. conyzoides* extract and the synthesized AgNPs in comparison with a standard (acarbose)

Conclusion

Aqueous leaf extract of *Ageratum conyzoides* reduced silver ions to silver nanoparticles, which possess considerable antioxidant, anti-inflammatory, and α-glucosidase inhibitory properties. Silver nanoparticles synthesized using *Ageratum conyzoides* extract should be further researched for its potential development as an antidiabetic agent.

Disclosure Statement

No potential conflict of interest was reported by the authors.

Funding

This research did not receive any specific grant from funding agencies in the public, commercial, or not-for-profit sectors.

Authors' Contributions

All authors contributed to data analysis, drafting, and revising of the paper and agreed to be responsible for all the aspects of this work.

Orcid

Jimoh Olamilekan Igbalaye
https://orcid.org/0000-0002-6690-4243
Adesegun Gideon Adeyemo
https://orcid.org/0000-0002-3421-5814

References

[1]. a) Nahar K., Rahaman M., Khan G.M.A., Islam M., Al-Reza S.M. *Asian J. Green Chem.,* 2021, **5**:135 [Crossref], [Google Scholar], [Publisher]; b) Zaid Almarbd Z., Mutter Abbass N. *Chemical Methodologies*, 2022, **6**:940 [Crossref], [Publisher]; c) Flayyih A.O., Mahdi W.K., Abu Zaid Y.I.M., Musa F.H. *Chemical Methodologies*, 2022, **6**:620 [Crossref], [Publisher]; d) Ikhioya I., Akpu N.I., Onoh E., Aisida S.O., Ahmad I., Maaza M., Ezema F. *Journal of Medicinal and Nanomaterials Chemistry*, 2023, **5**:156 [Crossref], [Publisher]; e) Sajjadnejad M., Haghshenas S.M.S. *Journal of Medicinal and Nanomaterials Chemistry*, 2023, **5**:69 [Crossref], [Publisher]; f) Hajinasiri R., Esmaeili Jadidi M. *Journal of Applied Organometallic Chemistry*, 2022, **2**:101 [Crossref], [Publisher]; g) Rostamzadeh Mansour S., Sohrabi-Gilani N., Nejati P. *Advanced Journal of Chemistry, Section A*, 2022, **5**:31 [Crossref], [Publisher]; h) Sharma M.,

Yadav S., Srivastava M., Ganesh N., Srivastava S. *Journal of Medicinal and Nanomaterials Chemistry*, 2022, **4**:313 [Crossref], [Publisher]; Khazaei R., Khazaei A., Nasrollahzadeh M. *Journal of Applied Organometallic Chemistry*, 2023, **3**:123 [Crossref], [Publisher]
[2]. a) Shaikh R., Nayab J., Shaikh N. *Asian J. Green Chem.,* 2021, **5**:313 [Crossref], [Google Scholar], [Publisher]; b) koohzadi N., Rezayati Zad, Z. *Adv. J. Chem. Sect. B. Nat. Prod. Med. Chem.*, 2021, **3**:311 [Crossref], [Publisher]
[3]. Li Y., Leung P., Yao L., Song Q.W., Newton E. *J. Hosp. Infect.,* 2006, **62**:58 [Crossref], [Google Scholar], [Publisher]
[4]. Prabhu S., Poulose E.K. *Int. Nano Lett.,* 2012, **2**:1 [Crossref], [Google Scholar], [Publisher]
[5]. Kayode Awote O., Solomon Anagun O., Gideon Adeyemo A., Olamilekan Igbalaye J., Lawrence Ogunc M., Kolawole Apete S., Oluwaranti Folami S., Esther Olalero F., Chidera Ebube S., Ishola Taofeeq M., Oluwapelumi Akinloye O. *Asian Journal of Green Chemistry*, 2022, **4**:284 [Crossref], [Publisher]
[6]. Lansdown A.B. *Curr. Probl. Dermatol.,* 2006, **33**:17 [Crossref], [Google Scholar], [Publisher]
[7]. Atiyeh B.S., Costagliola M., Hayek S.N., Dibo S.A. *Burns,* 2007, **33**:139 [Crossref], [Google Scholar], [Publisher]
[8]. Lansdown A.B.G. *Crit. Rev. Toxicol.,* 2007, **37**:237 [Crossref], [Google Scholar], [Publisher]
[9]. Ameer F.S., Varahagiri S., Benza D.W., Willett D.R., Wen Y., Wang F., Chumanov G., Anker J.N. *J. Phys. Chem. C. Nanomater. Interfaces,* 2016, **120**:20886 [Crossref], [Google Scholar], [Publisher]
[10]. Gan P.P., Li S.F. *Rev. Environ. Sci. Biotechnol.,* 2012, **11**:169 [Crossref], [Google Scholar], [Publisher]
[11]. Rafique M., Sadaf I., Rafique M.S., Tahir M.B. *Artif. Cells Nanomed. Biotechnol.,* 2017, **45**:1272 [Crossref], [Google Scholar], [Publisher]
[12]. Kuppusamy P., Yusoff M.M., Maniam G.P., Govindan N. *Saudi Pharm. J.,* 2016, **24**:473 [Crossref], [Google Scholar], [Publisher]
[13]. Chandraker S.K., Ghosh M.K., Lal M., Ghorai T.K. *New J. Chem.,* 2019, **43**:18175[Crossref], [Google Scholar], [Publisher]
[14]. Pourbahar N., Alamdar S. S. *Asian J. Green Chem.,* 2023, **7**:9 [Crossref], [Google Scholar], [Publisher]
[15]. Das R.K., Brar S.K. *Nanoscale,* 2013, **5**:10155 [Crossref], [Google Scholar], [Publisher]
[16]. Liu H., Hao C., Zhang Y., Yang H., Sun R. *Colloids Surf. B: Biointerfaces.,* 2021, **202**:111688 [Crossref], [Google Scholar], [Publisher]
[17]. Akintelu S.A., Bo Y., Folorunso A.S. *J. Chem.,* 2020, **2020**:3189043 [Crossref], [Google Scholar], [Publisher]
[18]. Okunade A.L. *Fitoterapia,* 2002, **73**:1 [Crossref], [Google Scholar], [Publisher]
[19]. Egunyomi A., Gbadamosi I.T., Animashahun M.O. *J. Med. Plants Res*., 2011, **5**:5347 [Google Scholar], [Publisher]
[20]. Ashour A.A., Raafat D., El-Gowelli H.M., El-Kamel A.H. *Int. J. Nanomedicine,* 2015, **10**:7207 [Google Scholar], [Publisher]
[21]. Fafal T.U., Taştan P.E., Tüzün B.S., Ozyazici M., Kivcak B. *S. Afr. J. Bot.,* 2017, **112**:346 [Crossref], [Google Scholar], [Publisher]
[22]. Keshari A.K., Srivastava A., Verma A.K., Srivastava R. *Br. J. Pharm. Res.,* 2016, **14**:1 [Crossref], [Google Scholar], [Publisher]
[23]. Oyedapo O.O., Famurewa A.J. *Int. J. Pharmacogn.,* 1995, **33**:65 [Crossref], [Google Scholar], [Publisher]
[24]. Juvekar A., Sakat S., Wankhede S., Juvekar M., Gambhire M. *Planta Med*., 2009, **75**:PJ178 [Crossref], [Google Scholar], [Publisher]
[25]. Varghese T., Mathew S. *J. Food Sci. Technol.,* 2017, **54**:2512 [Crossref], [Google Scholar], [Publisher]
[26]. Kim Y.M., Jeong Y.K., Wang M.H., Lee W.Y., Rhee H.I. *Nutrition,* 2005, **21**:756 [Crossref], [Google Scholar], [Publisher]
[27]. Carrillo C., Cavia M.M., Alonso-Torre S.R. *Nutr. Hosp.,* 2012, **27**:978 [Crossref], [Google Scholar], [Publisher]
[28]. Carrillo C., Cavia M.M., Alonso-Torre S.R. *Nutr. Hosp.,* 2012, **27**:1860 [Crossref], [Google Scholar], [Publisher]
[29]. Govindappa M., Hemashekhar B., Arthikala M.K., Rai V.R., Ramachandra Y.L.

Results Phys., 2018, **9**:400 [Crossref], [Google Scholar], [Publisher]
[30]. Sahu N., Soni D., Chandrashekhar B., Satpute D.B., Saravanadevi S., Sarangi B.K., Pandey R.A. *Int. Nano Lett.,* 2016, **6**:173 [Crossref], [Google Scholar], [Publisher]
[31]. Mock J.J., Barbic M., Smith D.R., Schultz D.A., Schultz S. *J. Chem. Phys.,* 2002, **116**:6755 [Crossref], [Google Scholar], [Publisher]
[32]. Subramanian R., Subbramaniyan P., Raj V. *Springerplus,* 2013, **2**:1 [Crossref], [Google Scholar], [Publisher]
[33]. Ibrahim H.M.M. *J. Radiat. Res. Appl. Sci.,* 2015, **8**:265 [Crossref], [Google Scholar], [Publisher]
[34]. Küp F.Ö., Çoşkunçay S., Duman F. *Mater. Sci. Eng. C.,* 2020, **107**:110207 [Crossref], [Google Scholar], [Publisher]
[35]. Keshari A.K., Srivastava R., Singh P., Yadav V.B., Nath G. *J. Ayurveda Integr. Med.,* 2020, **11**:37 [Crossref], [Google Scholar], [Publisher]
[36]. Chick C.N., Misawa-Suzuki T., Suzuki Y., Usuki T. *Bioorg. Med. Chem. Lett.,* 2020, **30**:127526 [Crossref], [Google Scholar], [Publisher]
[37]. Bharathi D., Bhuvaneshwari V. *Bionanoscience,* 2019, **9**:155 [Crossref], [Google Scholar], [Publisher]
[38]. Moldovan B., David L., Achim M., Clichici S., Filip G.A. *J. Mol. Liq.,* 2016, **221**:271 [Crossref], [Google Scholar], [Publisher]
[39]. Rajkumar T., Sapi A., Das G., Debnath T., Ansari A., Patra J.K. *J. Photochem. Photobiol. B, Biol.,* 2019, **193**:1 [Crossref], [Google Scholar], [Publisher]
[40]. Puntarulo S. *Mol. Asp. Med.,* 2005, **26**:299 [Crossref], [Google Scholar], [Publisher]
[41]. Ransy C., Vaz C., Lombès A., Bouillaud F. *Int. J. Mol. Sci.,* 2020, **21**:9149 [Crossref], [Google Scholar], [Publisher]
[42]. Valgimigli L., Baschieri A., Amorati R. *J. Mater. Chem. B.,* 2018, **6**:2036 [Crossref], [Google Scholar], [Publisher]
[43]. Kedi P.B., Meva F.E., Kotsedi L., Nguemfo E.L., Zangueu C.B., Ntoumba A.A., Mohamed H.E., Dongmo A.B., Maaza M. *Int. J. Nanomedicine,* 2018, **13**:8537 [Google Scholar], [Publisher]
[44]. Prabakaran A.S., Mani N. *J. Pharmacogn. Phytochem.,* 2019, **8**:2556 [Google Scholar], [Publisher]
[45]. Liu H., Hao C., Zhang Y., Yang H., Sun R. *Colloids Surf. B: Biointerfaces,* 2021, **202**:111688 [Crossref], [Google Scholar], [Publisher]
[46]. Jain A., Anitha R., Rajeshkumar S. J. *Res. J. Pharm. Technol.,* 2019, **12**:2790 [Crossref], [Google Scholar], [Publisher]
[47]. Ghani U., Nur-e-Alam M., Yousaf M., Ul-Haq Z., Noman O.M., Al-Rehaily A.J. *Bioorg. Chem.,* 2019, **87**:736 [Crossref], [Google Scholar], [Publisher]
[48]. Senthilkumar P., Santhosh Kumar D.R., Sudhagar B., Vanthana M., Parveen M.H., Sarathkumar S., Thomas J.C., Mary A.S., Kannan C. *J. Nanostructure Chem.,* 2016, **6**:275 [Crossref], [Google Scholar], [Publisher]
[49]. Jini D., Sharmila S. *Mater. Today: Proc.,* 2020, **22**:432 [Crossref], [Google Scholar], [Publisher]
[50]. Verma S., Hussain M.E. *Diabetes & Metabolic Syndrome: Clin. Res. Rev.,* 2017, **11**:73 [Crossref], [Google Scholar], [Publisher]
[51]. Alam F., Shafique Z., Amjad S.T. *Phytother. Res.,* 2019, **33**:41 [Crossref], [Google Scholar], [Publisher]

How to cite this manuscript: Jimoh Olamilekan Igbalaye*, Adesegun Gideon Adeyemo, Adetola Olajumoke Adenubi, Oladejo Ahmodu, Basit Opeyemi Shodimu, Faizat Olasumbo Hazeez, Suliat Adenike Hassan. Silver Nanoparticles Synthesized Using *Ageratum conyzoides* Leaf Extract Exhibit Antioxidant, Anti-inflammatory and α-Glucosidase Inhibitory Properties. *Asian Journal of Green Chemistry*, 8(4) 2024, 25-38. DOI: 10.48309/ajgc.2024.399046.1396